

Contents lists available at ScienceDirect

Petroleum Science

journal homepage: www.keaipublishing.com/en/journals/petroleum-science



Original Paper

Natural fractures and their effectiveness in deep tight sandstone reservoirs of foreland thrust belts in the southern Junggar Basin, China



Guo-Ping Liu ^{a, b}, Zhi-Jun Jin ^{a, *}, Lian-Bo Zeng ^{a, c}, Xiao-Xuan Chen ^d, Mehdi Ostadhassan ^e, Zhe Mao ^c, Jian-Kang Lu ^c, Song Cao ^c

- ^a Institute of Energy, Peking University, Beijing, 100871, China
- ^b School of Energy Resources, China University of Geosciences (Beijing), Beijing, 100083, China
- ^c College of Geosciences, China University of Petroleum (Beijing), Beijing, 102249, China
- ^d Xinjiang Oilfield Company, PetroChina, Karamay, 834000, Xinjiang, China
- ^e Key Laboratory of Continental Shale Hydrocarbon Accumulation and Efficient Development, Ministry of Education, Northeast Petroleum University, Daqing, 163318, Harbin, China

ARTICLE INFO

Article history: Received 14 March 2024 Received in revised form 27 September 2024 Accepted 1 April 2025 Available online 11 April 2025

Edited by Jie Hao and Meng-Jiao Zhou

Keywords:
Natural fractures
Effectiveness
Tectonism and diagenesis
Deep tight sandstone reservoirs
Foreland thrust belts

ABSTRACT

Strong tectonic activities and diagenetic evolution encourage the development of natural fractures as typical features in deep tight sandstone reservoirs of foreland thrust belts. This study focused on the Jurassic in the southern Junggar Basin to comprehensively analyze the fracture characteristics and differential distribution and, ultimately, addressed the controlling mechanisms of tectonism and diagenesis on fracture effectiveness. Results revealed that the intensity of tectonic activities determines the complexity of tectonic fracture systems to create various fracture orientations when they have been stronger. The intense tectonic deformation would impact the stratum occurrence, which results in a wide range of fracture dip angles. Moreover, as the intensity of tectonic activities and deformations weakens, the scale and degree of tectonic fractures would decrease continuously. The control of tectonism on fracture effectiveness is reflected in the notable variations in the filling of multiple group fractures developed during different tectonic activity periods. Fractures formed in the early stages are more likely to be filled with minerals, causing their effectiveness to deteriorate significantly. Additionally, the strong cementation in the diagenetic evolution can cause more fractures to be filled with minerals and become barriers to fluid flow, which is detrimental to fracture effectiveness. However, dissolution is beneficial in improving their effectiveness by increasing fracture aperture and their connectivity to the pores. These insights can refine the development pattern of natural fractures and contribute to revealing the evolutionary mechanisms of fracture effectiveness in deep tight sandstone reservoirs of foreland thrust belts. © 2025 The Authors. Publishing services by Elsevier B.V. on behalf of KeAi Communications Co. Ltd. This is an open access article under the CC BY license (http://creativecommons.org/licenses/by/4.0/).

1. Introduction

Deep reservoirs in foreland thrust belts are important for petroleum exploration and development, and many such reservoirs have been discovered worldwide, including the Western Canadian Sedimentary Basin, Neuquén Basin in Argentina, Rocky Mountain Front in the United States, Southern Junggar Basin in China, Sub-Andean Zone in South America, and elsewhere (Machel et al., 1996; Branellec et al., 2015; Eude et al., 2015; Bush et al., 2016; Liu et al., 2020b). These deep reservoirs are comprised of rocks

* Corresponding author.

E-mail address: jinzj1957@pku.edu.cn (Z.-J. Jin).

Peer review under the responsibility of China University of Petroleum (Beijing).

buried at depths exceeding 3500 m, which typically makes reservoirs tight, with generally poor reservoir properties (Ehrenberg and Nadeau, 2005; Liu et al., 2020a, 2020b). In addition, these reservoirs in foreland thrust belts usually experience multiple periods of complex and intense tectonic activities (Zhang et al., 2014; Chapman and Chapman, 2015; Feng et al., 2021). Except for the development of thrust faults and fault-related folds, the widespread development of natural fractures is a primary feature of these reservoirs (Hernandez and Franzese, 2017; Mao et al., 2022).

Natural fractures in foreland thrust belt reservoirs usually exhibit multiple stages of formation, while if they are developed prior to hydrocarbon accumulation, they will become major migration pathways affecting the distribution of such reservoirs, while those formed at the latter stages would control the

hydrocarbon preservation and petrophysical properties of reservoirs (Rachinskiy et al., 2007; Hernandez and Franzese, 2017; Liu et al., 2018; Kerimov et al., 2019; Lai et al., 2023a,b). Since deep reservoirs are commonly characterized by low matrix porosity and permeability, natural fractures can become a portion of the storage space and significantly increase reservoir permeability by serving as the fluid flow pathway (Ehrenberg and Nadeau, 2005; Ding et al., 2012; Selvadurai et al., 2018). Furthermore, natural fractures would affect the propagation and distribution of artificial fractures during hydraulic fracturing in deep tight sandstone reservoirs, thereby controlling the production as well (Warpinski and Teufel, 1987; Wang and Liu, 2021). Considering what was said, an in-depth investigation of natural fractures would be of great significance in effectively exploiting deep tight sandstone reservoirs in foreland thrust belts, which necessitates further research.

The intense tectonic activity and deformation varieties have caused the distribution of natural fractures to have strong heterogeneity in foreland thrust belts (Ajdukiewicz et al., 2010; Zhang et al., 2014; Gomez-Rivas et al., 2020; Mao et al., 2020). Published literature mainly focuses on the development patterns of natural fractures in structural areas and typical structures such as faults and folds, while research on the differential distribution of fractures in the whole foreland thrust belts is relatively scarce (Cardozo et al., 2005; Hannah et al., 2015; Cai et al., 2016; Zeng et al., 2016; Ju et al., 2018). Moreover, deep tight sandstone reservoirs in foreland thrust belts usually have undergone complex diagenetic processes, including strong compaction, pressure solution, and dominant cementation (Wierzbicki et al., 2006; Wang et al., 2019; Liu et al., 2021; Zhu et al., 2022). Consequently, multiple periods of tectonic activities and deformations in foreland thrust belts and the complex diagenesis experienced by deep tight sandstone reservoirs would make evaluating natural fractures and their effectiveness even more challenging.

The foreland thrust belt of the southern Junggar Basin is a hydrocarbon-enriched system adjacent to the Tianshan orogen, with significant economic potential for petroleum exploration and development (Cao et al., 2010; Guan et al., 2016). Among them, the Jurassic is predominantly composed of sandstones, most of which are buried deeper than 3500 m and some are beyond 6000 m, and is one of the principal strata for oil and gas accumulation (Clayton et al., 1997; Hu et al., 2010). The intense tectonic movements from the Yanshan to Himalayan stages created a zoned structural pattern in the southern Junggar Basin, where faults, anticlines, and natural fractures are widely developed (Ju et al., 2012; Wan et al., 2015; Liu et al., 2020b; Mao et al., 2022). By observing outcrops, cores, and thin sections, this study identified natural fractures in the Jurassic tight sandstone reservoirs in the foreland thrust belt and analyzed their development characteristics and differential distribution. Ultimately, this study discussed the control of tectonism and diagenesis on fracture effectiveness in these reservoirs. Results from this study may reveal the development pattern of natural fractures and the mechanisms controlling their effectiveness in deep tight sandstone reservoirs of foreland thrust belts.

2. Geologic setting

2.1. Location and structure

The Junggar Basin, located in northwestern China, is a sizeable petroliferous basin inside the continental plate that was formed during the Mesozoic (Fig. 1(a)). This basin has experienced three stages of tectonic evolution since the Permian, including the peripheral foreland basin in the Early Permian, the intracontinental depression from the Late Permian to Cretaceous, and the paraforeland basin from the Paleogene to Quaternary (Wan et al.,

2015; Liu et al., 2020b). The southern Junggar Basin, a secondary structural unit of the Junggar Basin, is adjacent to the Tianshan orogen in the south and belongs to the foreland thrust belt (Fig. 1(b) and (c)). Its long axis strikes NWW-SEE, about 650 km from east to west and 40-90 km from north to south, and covers an area of about 3.0×10^4 km² (Sun et al., 2004).

The Tianshan orogen compressed the southern Junggar Basin during the basin evolution, and the strong tectonic activities resulted in the formation of multiple structural units in the foreland thrust belt with various evolutionary characteristics (Fig. 1(c)). According to the structural features, the foreland thrust belt is divided into the western, middle, and eastern sections, with the severity of tectonic deformations gradually increasing (Fig. 2). It can also be divided into three structural zones from the Tianshan orogen to the interior Junggar Basin. For example, the middle section is divided into Oigu, Homatu, and Hu'an structural zones from south to north, and their deformation strengths gradually decrease. In the Cenozoic, the southern Junggar Basin underwent significant tectonic activities, resulting in a series of thrust faults and fault-related anticlines in the southern Junggar Basin (Guo et al., 2011; Guan et al., 2016). These faults are generally oriented in NW-SE directions and typically have high-dip angles (Yu et al., 2009). The anticlines are usually elongated and oriented parallel to the strikes of major faults, and some exhibit asymmetrical fold geometries while others are overturned (Mao et al., 2022).

2.2. Stratigraphy

The southern lunggar Basin exhibits foreland characteristics from the Permian to the Neogene and has deposited a thick sequence of multiple cycles of terrestrial strata (Yang et al., 2015; Zhang et al., 2022). The target layer of this study is the Mesozoic Jurassic, which exhibits a significant variation in burial depth, with a concentration greater than 3500 m and a maximum exceeding 6000 m (Mao et al., 2022). The Jurassic is composed of the Badaowan (J_1b), Sangonghe (J_1s), Xishanyao (J_2x), Toutunhe (J_2t), Qigu (J_3q) , and Kalazha (J_3k) formations from bottom to top (Fig. 3) (Qiu et al., 2021). The Lower Jurassic (J_1) is characterized by sedimentary facies ranging from braided rivers to shore-shallow lakes and braided river deltas (Liu et al., 2020b). The lower part (J_1b) is composed of interbedded fine sandstone, conglomerate, mudstone, and coal with irregular rhythmic layers, while the upper part (J_1s) is characterized by thick layers of fine sandstone, as well as some mudstone and sandstone conglomerate. The Middle Jurassic (J₂) has sedimentary facies ranging from lakes and marshes to braided rivers (Li et al., 2004). The lower part (J_2x) is mainly composed of fine sandstone, mudstone, and coal, while the upper part (J_2t) is characterized by rhythmic interbedding of mudstone, sandstone, and sandstone conglomerate. The Upper Jurassic (J₃) is comprised of sedimentary facies of braided rivers, shore-shallow lakes, and alluvial fans (Guo et al., 2011). The Qigu Formation (I_3q) is mainly composed of medium sandstone and fine sandstone with a small amount of mudstone, while the Kalazha Formation (J_3k) is composed of conglomerate and sandstone conglomerate with locally occurring medium to coarse sandstone.

2.3. Reservoir

The storage space of the Jurassic sandstone reservoirs in the southern Junggar Basin is mainly composed of primary intergranular pores and secondary intergranular and intragranular dissolution pores, as well as some natural fractures, with a heterogenous distribution (Qiu et al., 2021). Due to prolonged deep burial and strong tectonic compression after Jurassic sedimentation, the pore spaces in the rock layers rapidly decrease, creating tight reservoirs

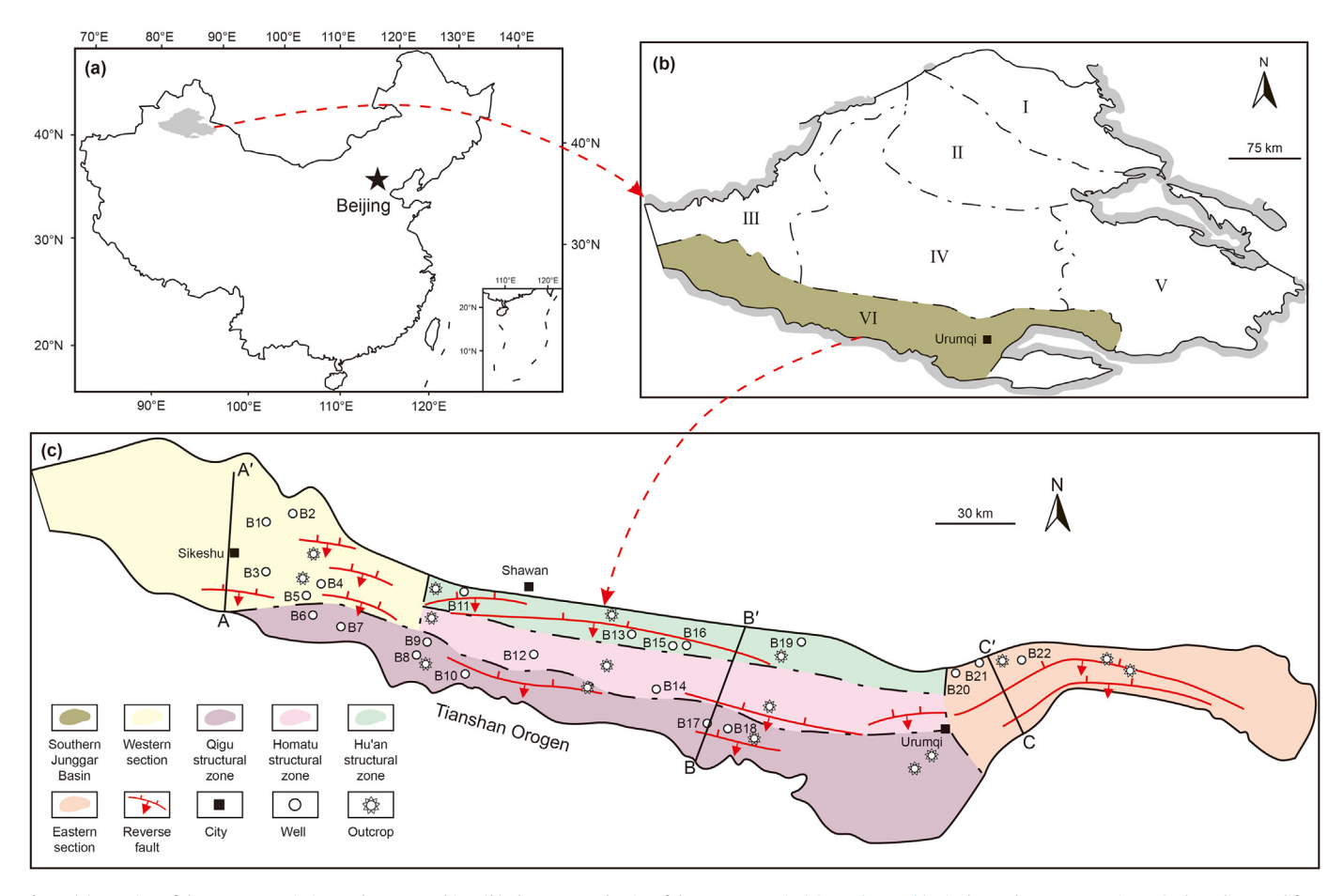


Fig. 1. (a) Location of the Junggar Basin in northwestern China. (b) The structural units of the Junggar Basin (Liu et al., 2020b). I is the Wulungu Depression. II is the Luliang Uplift. III is the Western Uplift. IV is the Central Depression Area. V is the Eastern Uplift. VI is the Southern Thrust Belt. (c) The map shows the foreland thrust belt of the southern Junggar Basin, including structural units, major faults, wells, outcrops, and the cross-sections in Fig. 2. The faults have been modified according to Yu et al. (2009).

(Zhang et al., 2020). The Lower (J₁) and Middle (J₂) Jurassic reservoirs are mainly composed of fine sandstones and siltstones, and under the influence of strong compaction and cementation, these reservoirs have limited storage space, with a porosity that is typically measured below 10% (Zhou et al., 2022). The Upper Jurassic (J₃) reservoirs primarily consist of medium-coarse sandstones and conglomerates, with a larger proportion of porosity greater than 10%. Except for the relatively high permeability of the Karazha Formation, the average air permeability of the reservoirs in other formations is less than 1 mD (Liu et al., 2020b). The intense tectonic activities of the foreland thrust belt have led to the widespread development of natural fractures in these reservoirs, which have been found to improve their permeability significantly (Mao et al., 2020). Overall, the petrophysical properties of the Jurassic in the southern Junggar Basin are poor, and they are recognized as deep tight sandstone reservoirs.

3. Data set and methodology

This study is based on the analysis of natural fractures and their development characteristics at different scales of investigation, with emphasis on the fracture parameter distribution and variation in the deep Jurassic tight sandstone reservoirs of the foreland thrust belt in the southern Junggar Basin. The observation and measured data of natural fractures are collected from analogous outcrops, cores, and thin sections in different structural units of the southern Junggar Basin. As shown in the map in Fig. 1(c), the analogous

outcrops are taken from 16 separate locations, all from the Jurassic sandstones that have experienced similar tectonic movements and diageneses with the subsurface strata. The core description was conducted on 496 m retrieved from 22 vertical wells, as shown in Fig. 1(c) in the Jurassic sandstone reservoirs. Thin sections (30 μm in thickness) of 83 samples from cores were impregnated with bluedye resin to highlight natural fractures and pores. Moreover, supporting information, including tectonic activities, structural characteristics, cross-sections, stratigraphy, lithology, porosity, and permeability, was obtained from the oilfield database and published literature.

Through the observation of natural fractures at outcrop, core, and thin section scales, this study identified fracture types and elucidated their development characteristics in deep tight sandstone reservoirs of foreland thrust belts. In order to investigate the distribution of natural fractures, fracture parameters, including the orientation, dip angle, scale, density, filling, and aperture, were quantitatively characterized (Hennings et al., 2000; Ortega et al., 2006; Ding et al., 2016; Liu et al., 2024). The scale of natural fractures refers to the height of macroscopic fractures and the extension length of microscopic fractures. The density of natural fractures in this study is linear density, which is the number of fractures per unit length (Laubach et al., 2009; Zeng and Li, 2009). It should be noted that these fracture parameters from analogous outcrops, cores, and thin sections may differ from those under formation temperature and pressure conditions and, therefore, are considered to have some limitations. However, this is a common

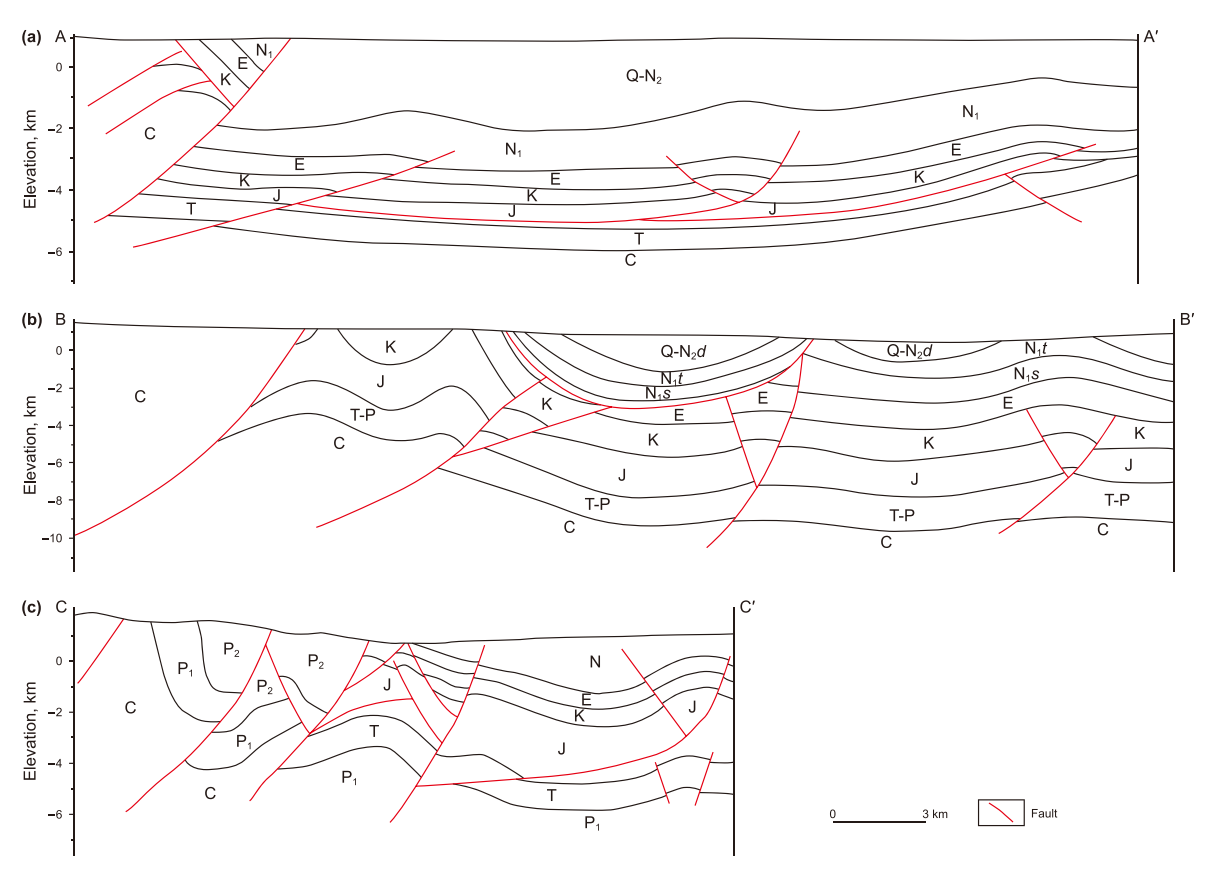


Fig. 2. The cross-sections of the western (a), middle (b), and eastern (c) sections in the thrust belt of the southern Junggar Basin (modified from Yu et al., 2009; Liu et al., 2020b). The position of these cross-sections is shown by A-A' (a), B-B' (b), and C-C' (c) in Fig. 1.

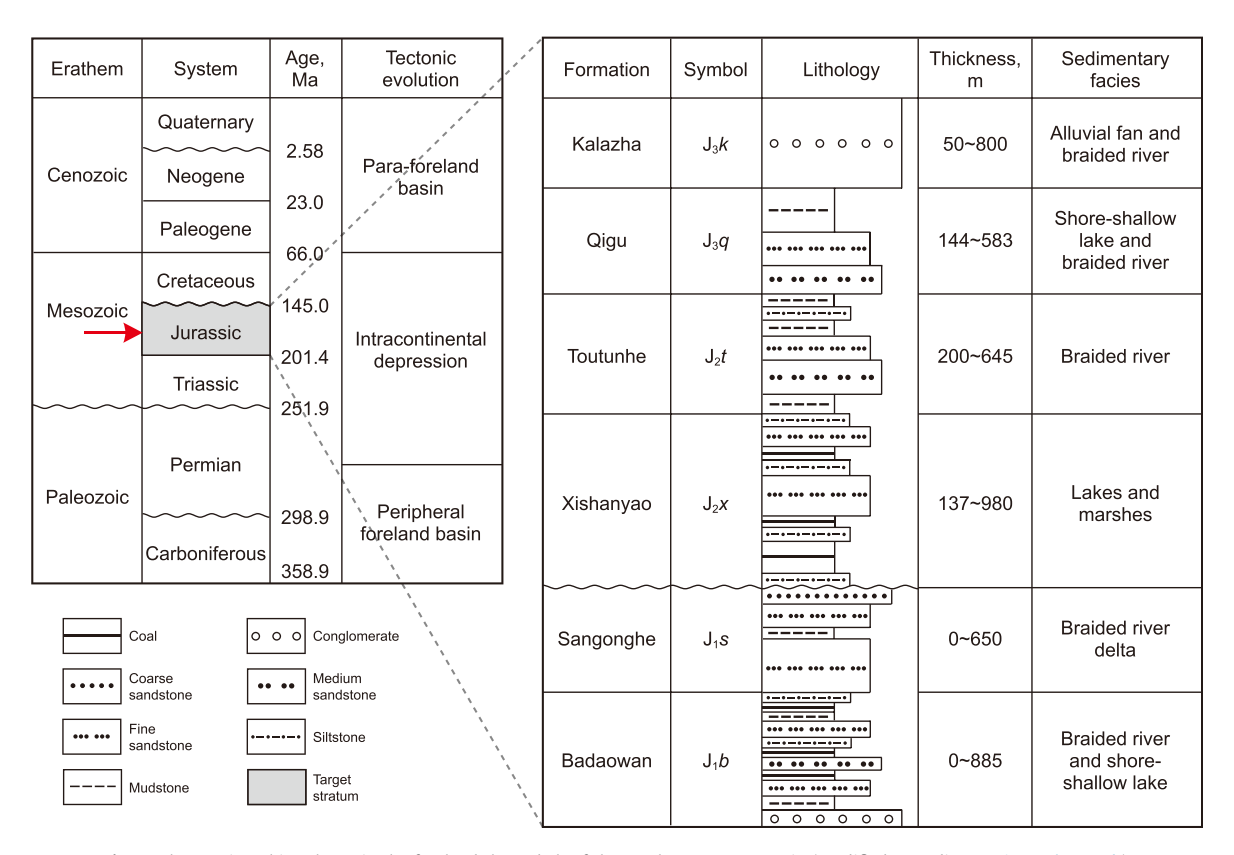


Fig. 3. The stratigraphic column in the foreland thrust belt of the southern Junggar Basin (modified according to Liu et al., 2020b).

challenge faced by reservoir fracture research, which usually has some effect on the aperture and less influence on other fracture parameters. This study focuses on the changes in fracture parameters, so the results are not substantially limited.

Based on the measured data of natural fractures from analogous outcrops, cores and thin sections, this study analyzed the variation of fracture parameters in these reservoirs of different structural units, attempting to explain the differential distribution of natural fractures developed in deep tight sandstone reservoirs of foreland thrust belts. In addition, this study investigated the various fracture fillings with respect to the tectonic activity stages as well as the effects of cementation and diagenesis on fracture filling and aperture. The ultimate aim was to explore the controlling mechanism of tectonism and diagenesis on fracture effectiveness in deep tight sandstone reservoirs within foreland thrust belts.

4. Results

4.1. Natural fracture types and characteristics

Based on outcrops, cores, and thin section observations, natural fractures in deep tight sandstone reservoirs of foreland thrust belts are divided into tectonic and non-tectonic fractures. Considering fracture mechanics, tectonic fractures are further classified into shear and extension fractures, while non-tectonic fractures mainly refer to those formed by compaction, dissolution, and subsurface fluid activities during the diagenetic evolution of the rocks (Aguilera, 1998; Ramsey and Chester, 2002; Zeng et al., 2010; Kus, 2017; Liu et al., 2020a). The target strata in this study area are located in the foreland thrust belt and have experienced multiple complex and intense tectonic deformation in their burial history (Guo et al., 2011; Guan et al., 2016). Consequently, tectonic fractures, especially the tectonic shear fractures, are the dominant type most ubiquitously developed in these reservoirs.

4.1.1. Tectonic fractures

In deep tight sandstones, macro-tectonic fractures are subdivided into translayer, layer-parallel, and intralayer fractures based on their occurrence (Figs. 4 and 5). The scale and dip angles of translayer fractures are large, while the layer-parallel and intralayer fractures have relatively small scales and variable dip angles controlled by the layer occurrence. Outcrops and cores suggest that the shear fractures in these rocks are dominated by intralayer fractures, with less development of translayer and layer-parallel fractures. These fractures are usually developed conjugately and appear in groups, and different groups exhibit a relationship of cutthrough or restricting each other (Fig. 5(b)). Shear fractures are relatively straight, and scratches and steps are occasionally developed on their surface (Fig. 5(a)–(c)). They also demonstrate some variation in different lithologies. In larger-grained rocks, such as conglomerate and coarse sandstone, shear fractures appear as distinct features of cutting through the grains (Fig. 5(e)). These fracture surfaces are relatively rough due to the presence of large grains in the matrix. In fine-grained rocks, especially those with more argillaceous content (such as mudstone and silty mudstone), the shear fracture surface is smoother and exhibits specular features with evidently developed scratches (Fig. 5(d) and (f)). Extension fractures are commonly observed in specific structural parts, such as the core of the anticline, and are less developed in such reservoirs. The surface of such fractures is uneven, and their extension is unstable (Fig. 5(g)).

Microscopic-scale tectonic fractures are also well developed in these sandstones of the foreland thrust belt, which are classified as transgranular, grain boundary, and intragranular fractures according to their relationship with mineral grains (Kranz, 1983; Zeng and Li, 2009). Transgranular fractures will pass through multiple mineral grains and extend longer (Fig. 6(a) and (b)). Grain boundary fractures are developed around the mineral grains, and their extension is primarily controlled by the grain shape (Fig. 6(c)). These fractures are usually interconnected in a network. Intragranular fractures are developed inside mineral grains, and they are distributed randomly in non-cleavage minerals such as quartz (Fig. 6(d) and (e)) but are more likely to grow along cleavage in cleavage minerals such as feldspar and calcite (Fig. 6(f)). The origin of the latter two micro-fractures might not be just tectonism, but also diageneses such as compaction and pressure solution (Laubach et al., 2010). Moreover, observations manifest that intragranular and grain boundary fractures are more accessible to develop when the mineral grains are larger, whereas transgranular fractures are less developed. It is speculated that the same tectonic stress would be more challenging to cut through larger mineral grains.

4.1.2. Non-tectonic fractures

Non-tectonic fractures are primarily comprised of bedding-parallel fractures and overpressure-related fractures in deep tight sandstones of foreland thrust belts. Bedding-parallel fractures are relatively straight and are usually developed along the depositional plane (Fig. 7(a) and (b)) (Liu et al., 2025). The lateral extension of these fractures is poor in tight sandstones, resulting in discontinuous distribution and varying lengths. Furthermore, these fractures will branch during their extension and bypass mineral grains rather than cut through them. Bedding-parallel fractures are mostly distributed in fine-grained rocks such as siltstone and argillaceous siltstone.

In addition, another type of fracture that is believed to form related to the overpressure of subsurface fluids is observed as well (Lyu et al., 2017; Meng et al., 2021). In the Jurassic tight sandstones of the foreland thrust belt in the southern Junggar Basin, there are significant overpressure systems with a formation pressure coefficient of up to 1.40-2.34 (Zhao, 2003; Hong et al., 2018). Herein, tectonic compressive stress and thick mudstone sealing are the main reasons for the formation of the reservoir overpressure (Gong et al., 2017). In the extruded tectonic settings, these fractures are generally lenticular, with relatively short extensions and large apertures (Fig. 7(c)). The occurrence of such fractures is unstable, and their distribution has no remarkable regularity. The unique geometry of these fractures is relevant to the stress conditions during the formation of ancient overpressure fluids. Normally, the fracture surface is perpendicular to the direction of the minimum principal stresses (Lyu et al., 2017). Mineral vein cement is a typical feature of overpressure-related fractures in deep tight sandstone reservoirs, mainly calcite and a small amount of bitumen. It's important to note that these fractures are relatively rarely developed in the study area.

4.2. Natural fracture distribution

Various sources of data state that the development and distribution of natural fractures show prominent heterogeneity in deep tight sandstone reservoirs in the foreland thrust belt of the southern Junggar Basin. In the eastern section of the foreland thrust belt, all tectonic fractures of the NEE-SWW and NW-SE strikes are well-developed in reservoirs, apart from the NNE-SSW striking fractures that are relatively poorly developed (Fig. 8(a)). Conversely, NNE-SSW striking fractures are more developed than other groups in the middle and western sections (Fig. 8(b) and (c)). Moreover, from the Tianshan orogen to the interior Junggar Basin, the dominant fracture orientations of tectonic fractures vary significantly in different structural zones of the foreland thrust belt (Fig. 8(d)—(f)). Overall, with the increased distance from the Tianshan orogen, the



Fig. 4. Macro-tectonic fractures in outcrops of the Jurassic tight sandstones in the southern Junggar Basin. TF in (a) is translayer fractures. IF in (b) is intralayer fractures.

group diversity of tectonic fractures tends to reduce, and their dominant orientations become more apparent. This proposes that the intensity of tectonic activities should be an essential factor leading to the complexity of the tectonic fracture system, hence such fractures have more diverse orientations when the tectonic deformation has been stronger (Zhang et al., 2017; Feng et al., 2018).

Additionally, because of the strong tectonic deformation, the target layers in this study area have grown many faults and anticlines with diverse striking fractures (Wan et al., 2015; Guan et al., 2016). When the position in these structures changes, the fracture groups will also be different, primarily due to the variations in the stress distribution and stratum occurrence (Sanz et al., 2008; Tavani et al., 2015). For example, near the fault, the translayer fractures with small angles or near parallel to the fault plane strike are more developed and are larger in scale (Fig. 9(a)), while those far away from the fault are mainly regional fractures that are less affected by the fault (Fig. 9(b)). In the anticline, fractures parallel to its axis are generally developed in the core, while in the wings, conjugate shear fractures become dominant (Watkins et al., 2015; Mao et al., 2022). Consequently, multiple periods of intense tectonic activities and

various types of structures are the crucial factors influencing the anisotropies of fracture strikes in reservoirs of foreland thrust belts.

Based on the dip angles, tectonic fractures are divided into five categories: near horizontal [0°, 3°], low dip angle (3°, 30°], medium dip angle $(30^\circ, 60^\circ]$, high dip angle $(60^\circ, 87^\circ]$, and near vertical $(87^\circ, 87^\circ]$ 90°] fractures (Zhang et al., 2023). Statistical data from core observations denote that the dip angle of tectonic fractures tends to increase gradually from the eastern to western sections of the southern Junggar Basin (Fig. 10(a)). Overall, the proportion of high dip angle and near vertical fractures increases, while that of the low to medium dip angle fractures decreases, and the overall proportion of near horizontal fractures becomes relatively small. Furthermore, in different structural zones of the middle section, the frequency of high dip to near vertical fractures increases from the near Tianshan orogen to the interior Junggar Basin (Fig. 10(b)). Specifically, the proportion of near horizontal to medium dip angle fractures in the Qigu structural zone near Tianshan orogen is higher. In contrast, in the Homatu and Hu'an structural zones, high dip to vertical fractures become more.

Observation and statistics explain that tectonic fractures in deep tight sandstone strata are primarily intralayer ones that intersect

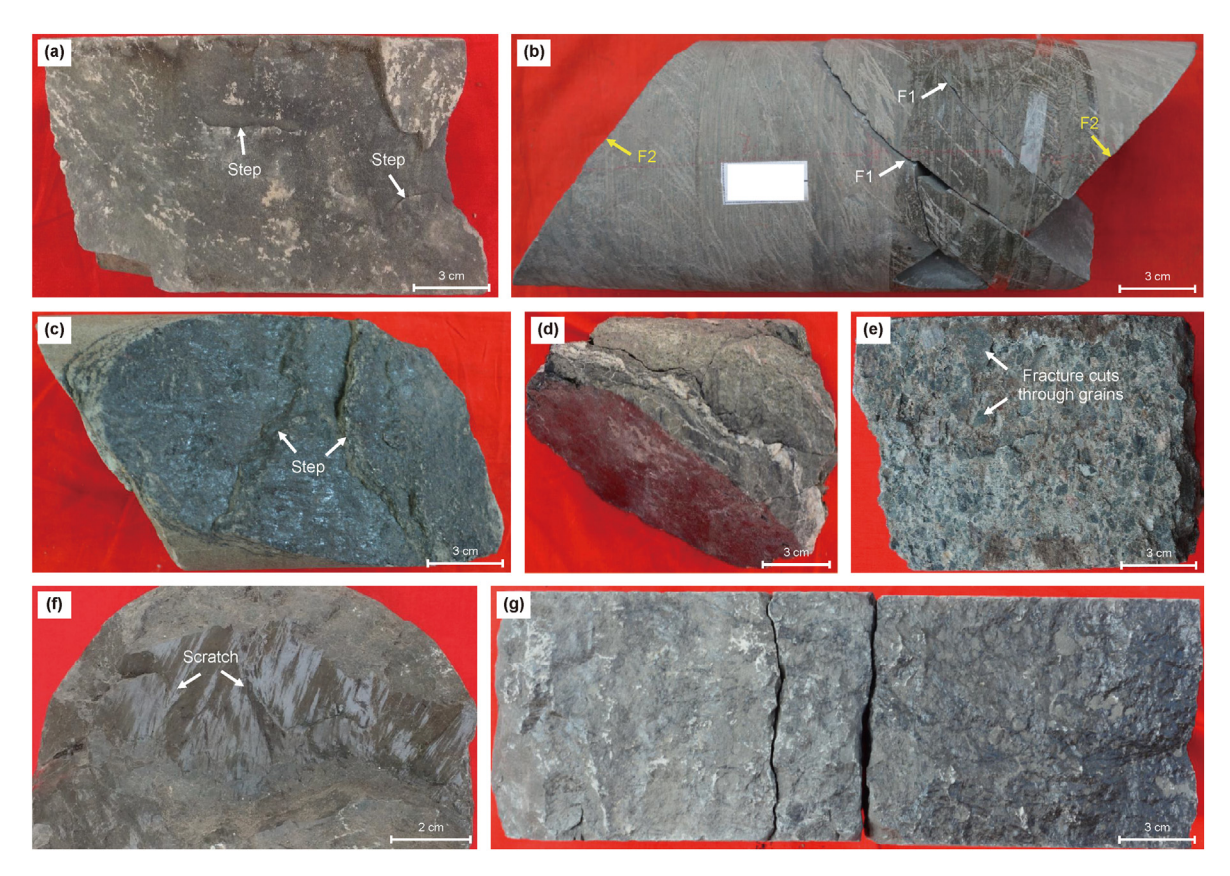


Fig. 5. Macro-tectonic fractures observed in cores retrieved from the Jurassic tight sandstone reservoirs in the southern Junggar Basin. (a) Intralayer fractures in Well B5, depth 5843.62 m. (b) Intralayer fractures in Well B21, depth 2067.98 m. Set F₁ restricted the extension of Set F₂. (c) Layer-parallel fractures in Well B5, depth 6414.01 m. (d) Layer-parallel fractures in Well B9, depth 1598.58 m. (e) Translayer fractures in Well B2, depth 4026.30 m. (f) Intralayer fractures in Well B3, depth 5423.28 m. (g) Intralayer fractures in Well B9, depth 485.57 m.

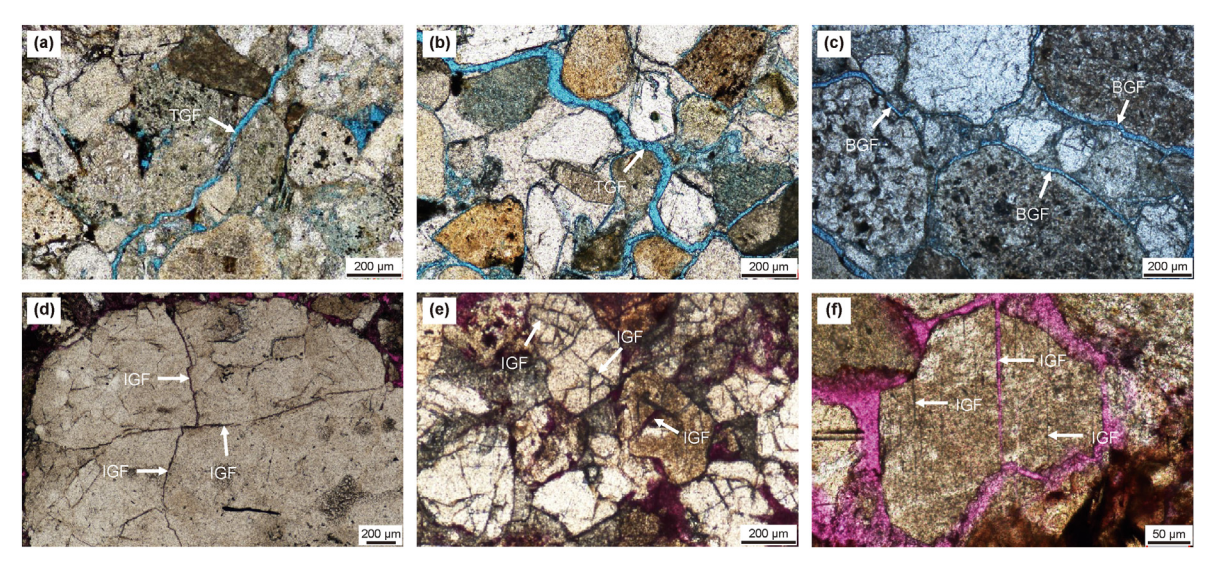


Fig. 6. Micro-tectonic fractures in thin sections of the Jurassic tight sandstone reservoirs in the southern Junggar Basin. (a) Transgranular fractures in Well B4, depth 4223.58 m. (b) Transgranular fractures in Well B14, depth 4628.06 m. (c) Grain boundary fractures in Well B6, depth 2492.89 m. (d) Intragranular fractures in Well B12, depth 4272.40 m. (e) Intragranular fractures in Well B17, depth 3106.20 m. (f) Intragranular fractures in Well B21, depth 2612.32 m. TGF is transgranular fractures. BGF is grain boundary fractures. IGF is intragranular fractures.

with the interface of the layers at a large angle or near vertical (Fig. 9(b)). In contrast, the layer-parallel fractures that intersect with the layer interface at lower angles are rarely observed. In foreland thrust belts, regional faults, anticlines, and other

structures are highly developed in areas primarily affected by tectonism, resulting in a larger dip angle of the stratum. Therefore, the dip angle of tectonic fractures decreases continuously with the increase of the dip angle of strata. Spanning from the eastern to

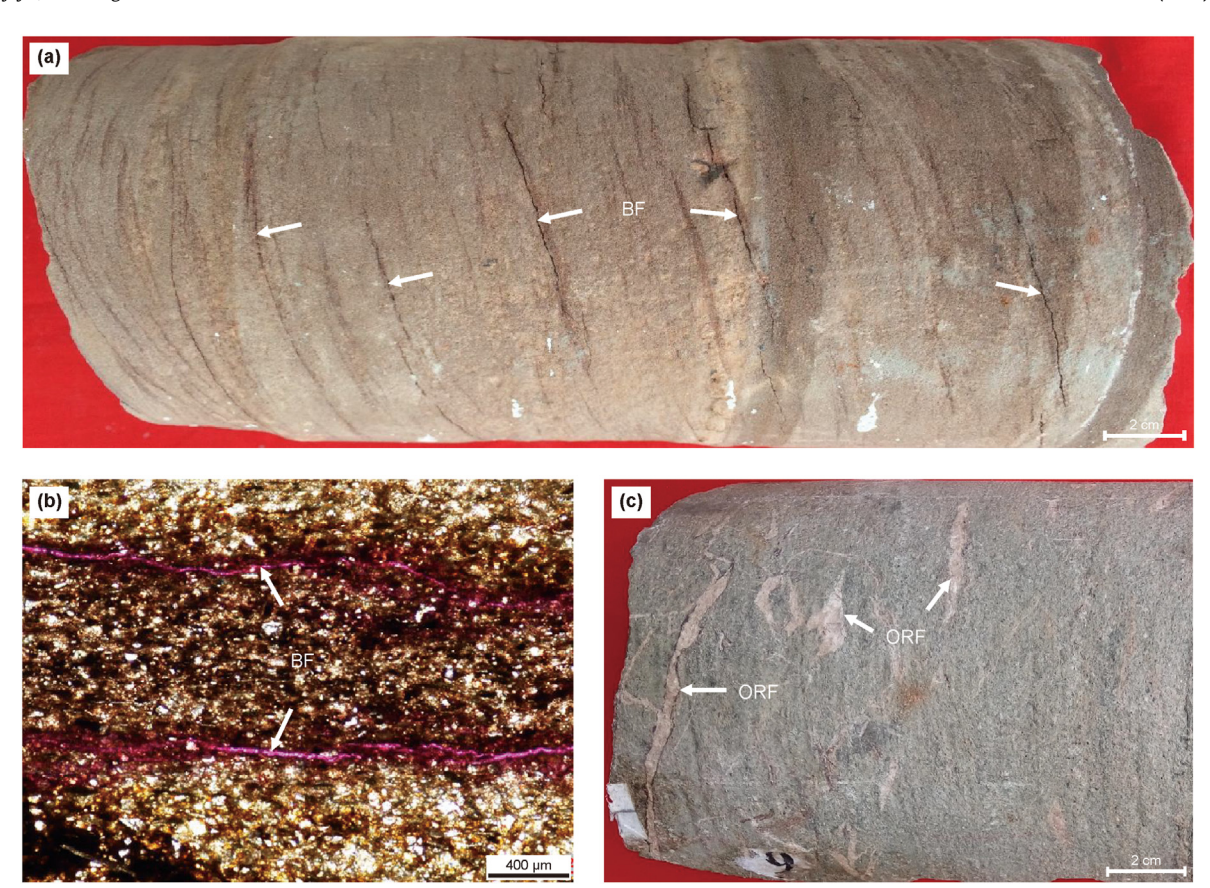


Fig. 7. Non-tectonic fractures in the Jurassic tight sandstone reservoirs of the southern Junggar Basin. (a) Bedding-parallel fractures in Well B11, depth 3346.58 m. (b) Bedding-parallel fractures in Well B13, depth 2429.10 m. (c) Overpressure-related fractures in Well B2, depth 4058.56 m. BF is bedding-parallel fractures. ORF is overpressure-related fractures.

western sections and extending from the near Tianshan orogen to the interior Junggar Basin, the intensity of tectonic activities and deformations are gradually weakened, which made the dip angle of the stratum decrease as well, resulting in the dip angle of fractures in these tight sandstone reservoirs to increase. In conclusion, the distribution of dip angles of these fractures is generally determined by the variations in the stratum occurrence resulting from the differential tectonic activities and structural features. This fundamental factor is also responsible for the wide range of dip angles of fractures observed in foreland thrust belts, in contrast to other regions where dip angles are predominantly high to near vertical.

Analysis from core observations corroborates that the scale of tectonic fractures decreases from the eastern to western section of the foreland thrust belt, explicitly showing that the proportion of tectonic fractures with a height less than 10 cm increases, whereas those larger than 10 cm decreases (Fig. 11(a)). Considering the middle section of the foreland thrust belt, the fracture scale displays a similar trend from the Tianshan orogen to the interior Junggar Basin (Fig. 11(b)). Notably, the Qigu structural zone exhibits a higher proportion of tectonic fractures with a height exceeding 10 cm, whereas the Homatu and Hu'an structural zones are characterized by a larger proportion of fractures generally less than 10 cm. This discrepancy in fracture scale is speculated to be influenced by variations in the intensity of tectonic deformations as a result of tectonism. In the southern Junggar Basin, from the eastern to western sections and from the Tianshan orogen to the interior Basin, a decreasing magnitude in tectonic activities is recorded, resulting in a continuous decrease in fracture scales.

Considering different sections in the southern Junggar Basin, tectonic fractures are more frequent in the eastern and middle sections, with an average linear density of more than 2.20 m⁻¹, but with limited development in the western section, where the average linear density is less than 1 m⁻¹ (Fig. 12(a)). Moreover, in the middle section of the foreland thrust belt, the Qigu structural zone has developed tectonic fractures with an average linear density of more than 3.00 m⁻¹, yet the Huomatu and Hu'an structural zones have relatively poor development of tectonic fractures, whose average linear density is less than 2.00 m^{-1} (Fig. 12(b)). This variation in the magnitude of the tectonic fracture development in foreland thrust belts can be attributed to the heterogeneity in the strength of tectonic deformation (Sanz et al., 2008; Eckert et al., 2014). In the southern Junggar Basin, which is severely affected by the formation and evolution of the Tianshan orogen, the tectonic activities in the eastern section are stronger, followed by the middle section and, finally, the western section. Synchronously, in the context of a foreland basin from a tectonic point of view, the Qigu structural zone, located close to the Tianshan orogen, has experienced significant tectonic deformation. However, as one moves toward the interior of the basin, the deformations in the Huomatu and Hu'an structural zones are rapidly weakened.

5. Discussion

The effectiveness of natural fractures is a crucial point in evaluating their impact on reservoirs, which determines the distribution of favorable reservoirs and the formulation of exploration and

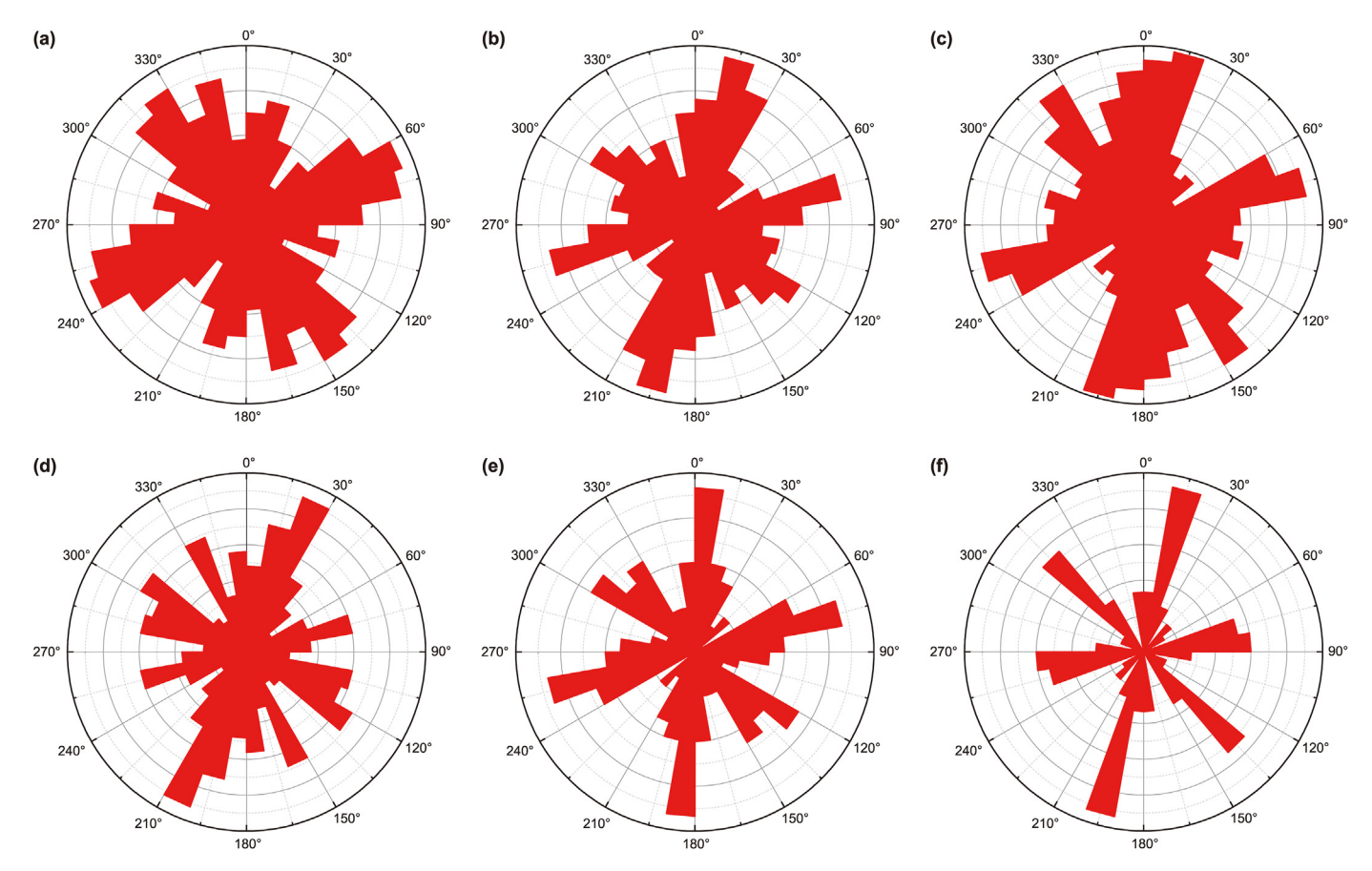


Fig. 8. Orientations of tectonic fractures from the Jurassic outcrops in different structural units of the southern Junggar Basin. (a) Eastern section (N = 440), (b) Middle section (N = 380), (c) Western section (N = 552), (d) Qigu structural zone (N = 212), (e) Homatu structural zone (N = 93), (f) Hu'an structural zone (N = 75). The location of these structural areas can be found in Fig. 1(c).

development plans in deep tight sandstone reservoirs in foreland thrust belts (Laubach et al., 2010; Azizmohammadi and Matthäi, 2017; Lahiri, 2021). During reservoir evolution, natural fractures can be filled with minerals and become barriers to fluid flow, causing their effectiveness to deteriorate significantly (Hood et al., 2003; Zeng et al., 2012). The filling degree of natural fractures is divided into complete-filled, half-filled, partial-filled, and unfilled, reflecting the sequential improvement of fracture effectiveness (Liu et al., 2021) (Fig. 13). Importantly, even fractures that are completefilled with minerals are not entirely ineffective for the reservoir, only indicating their effectiveness is relatively poor (Landry et al., 2016). Natural fractures with different scales in the Jurassic sandstones may be filled with minerals, and these minerals are mainly calcite, in addition to some bitumen and clay minerals (Liu et al., 2020b). The bitumen filling the fractures is formed by the precipitation of heavy components remaining after the light components of hydrocarbons are dispersed, representing the significant migration of fractures in hydrocarbon accumulation (Fig. 13(d)). The obvious hydrocarbon displayed on the fracture surface demonstrates these effective fractures serve as important flow conduits and storage space in these reservoirs (Fig. 13(e)).

Nearly 60% of tectonic fractures observed in the cores are unfilled and effective, while the complete-filled tectonic fractures account for about 20% and are the least effective. The proportion of partial-filled and half-filled tectonic fractures is around 10%, respectively, with relatively poor effectiveness. Furthermore, the interpretation of image logs also indicates tectonic fractures not filled by minerals account for a high proportion, reaching an

average of 69%. The width of mineral veins in filled tectonic fractures ranges from 0.5 mm to 5 mm, and their distribution is almost constant in a fracture. For non-tectonic fractures, bedding-parallel fractures are all effective fractures that are not filled with minerals. However, fractures related to overpressure of subsurface fluids are almost filled with minerals and have become relatively ineffective, with mineral veins that are usually wider than 2 mm and are non-uniform (Fig. 7(c)).

The foreland thrust belt usually has experienced multiple stages of intensive tectonic activities, resulting in the formation of diverse groups of tectonic fractures with complexity in deep tight sandstone reservoirs (Chapman and Chapman, 2015; Hernandez and Franzese, 2017). Core observation shows that multiple groups of tectonic fractures can be developed at the same place, some of which are filled with minerals while others are not (Fig. 14(a)). Outcrop investigation also reveals the filling regularity of tectonic fractures in different groups. When multiple groups of tectonic fractures are developed simultaneously, NW-SE striking fractures are more likely to be filled with minerals and to become ineffective (Fig. 14(b) and (c)). Statistical results from outcrops show NW-SE strike fractures account for more than 70% of mineral-filled tectonic fractures, while NEE-SWW and NNE-SSW striking fractures occupy much smaller proportions (Fig. 15). Consequently, these fractures in multiple groups exhibit different filling characteristics, which significantly alter their effectiveness.

Further analysis reveals that the NW-SE striking fractures in outcrops extend longer, while the NEE-SWW and NNE-SSW striking fractures are relatively short and usually exhibit conjugate



Fig. 9. Tectonic fractures in the Jurassic outcrops of the southern Junggar Basin. (a) F₁ is the large-scale tectonic fracture affected by the fault. (b) F₂ and F₃ are small-scale regional tectonic fractures.

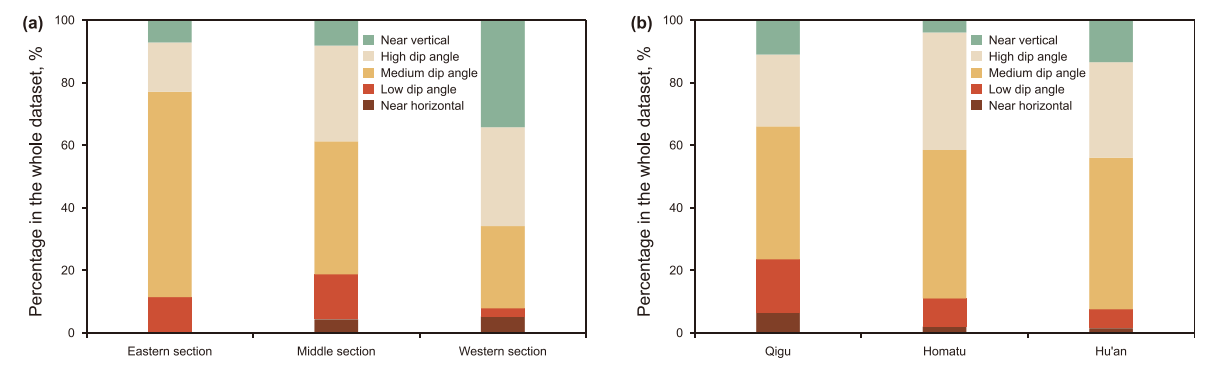
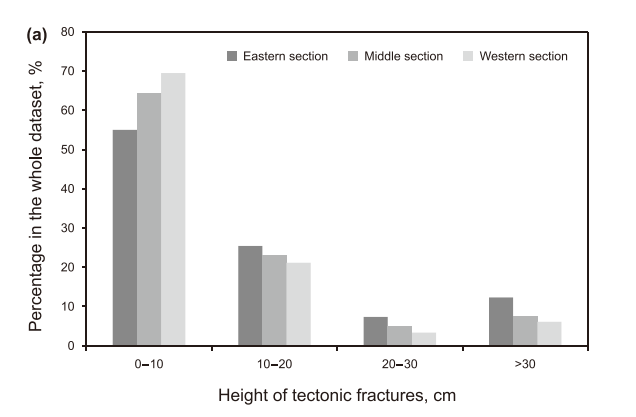


Fig. 10. The frequency of tectonic fractures with different dip angles from the Jurassic cores in various sections (a) and structural zones (b) of the southern Junggar Basin. The location of these structural areas is marked in Fig. 1(c).

characteristics. Moreover, NW-SE striking fractures restrict the extension of NEE-SWW and NNE-SSW strikes, reflecting that NW-SE striking fractures were formed in earlier tectonic activities (Fig. 14(b) and (c)). These suggest that NW-SE striking fractures have experienced more extended periods and more stages of fluid activity, as well as mineral precipitation and crystallization, compared with other groups of fractures (Hood et al., 2003; Gale et al., 2010). As a result, more NW-SE striking fractures are filled

with minerals, reducing their effectiveness. On the contrary, NEE-SWW and NNE-SSW striking fractures that are formed in later tectonic activities have experienced relatively less fluid activity, so they have a lower filling percentage and are generally more effective. Meanwhile, it should be emphasized that not all mineral-filled fractures are developed earlier, because regional fluids and abnormally high pressures can also promote the growth of minerals in fractures and fill them within a particular area (Fossen et al., 2007;



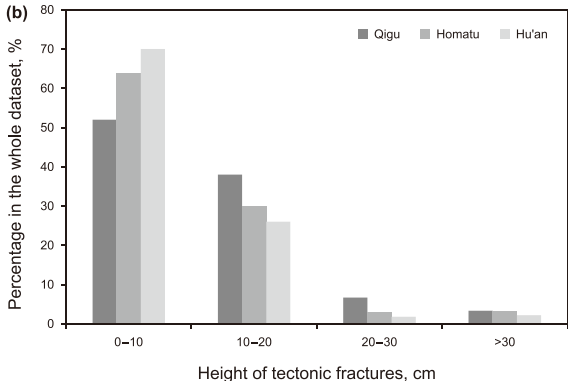
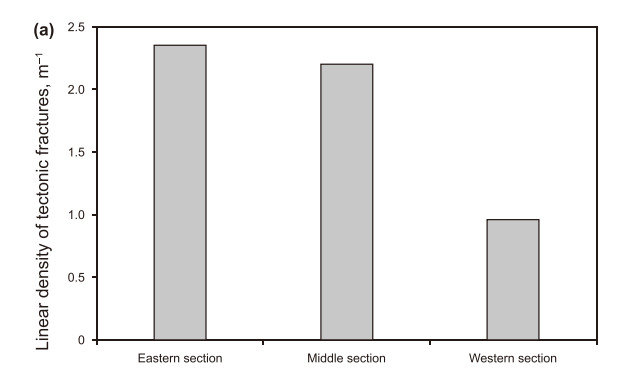


Fig. 11. The height of tectonic fractures from the Jurassic cores in different sections (a) and structural zones (b) of the southern Junggar Basin. The location of these structural areas is marked in Fig. 1(c).



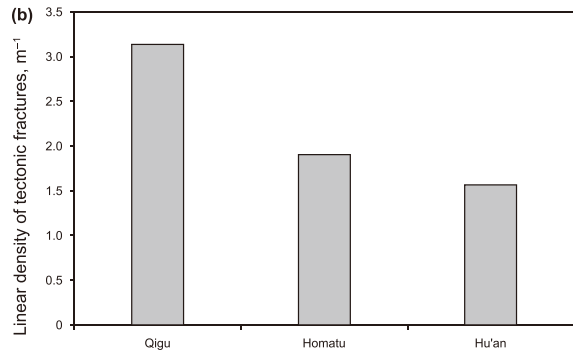


Fig. 12. The average linear density of tectonic fractures from the Jurassic cores in different sections (a) and structural zones (b) of the southern Junggar Basin. The location of these structural areas can be found in Fig. 1(c).

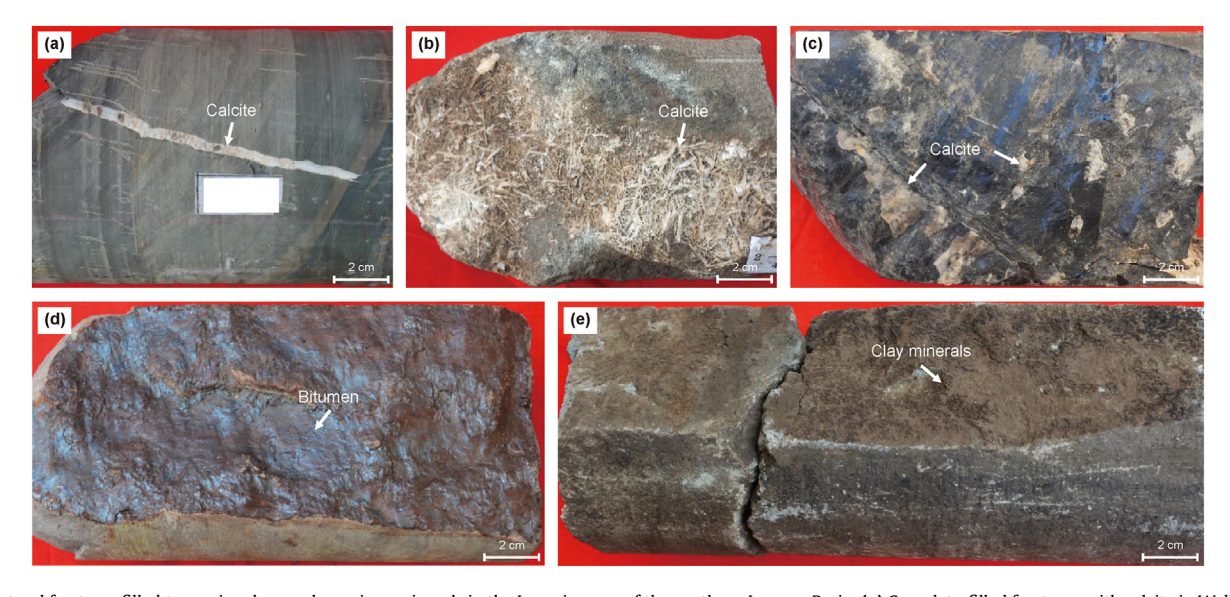


Fig. 13. Natural fractures filled to varying degrees by various minerals in the Jurassic cores of the southern Junggar Basin. (a) Complete-filled fractures with calcite in Well B3, depth 5412.74 m. (b) Half-filled fractures with calcite in Well B5, depth 6416.99 m. (c) Partial-filled fractures with calcite in Well B6, depth 2496.40 m. (d) Complete-filled fractures with bitumen in Well B1, depth 3412.06 m. (e) Partial-filled fractures with clay minerals in Well B2, depth 4030.12 m.

Eichhubl et al., 2009). Therefore, the control of tectonism on fracture effectiveness is reflected in the remarkable differences in the filling of multiple groups of tectonic fractures developed during different periods of tectonic activities. Fractures formed in earlier stages are more likely to be filled with minerals and become

ineffective, while those developed later are mostly unfilled and effective.

Deep tight sandstone reservoirs exhibit differences in diagenetic facies, which also lead to variations in natural fracture effectiveness. Due to data limitations, this study focuses on analyzing the

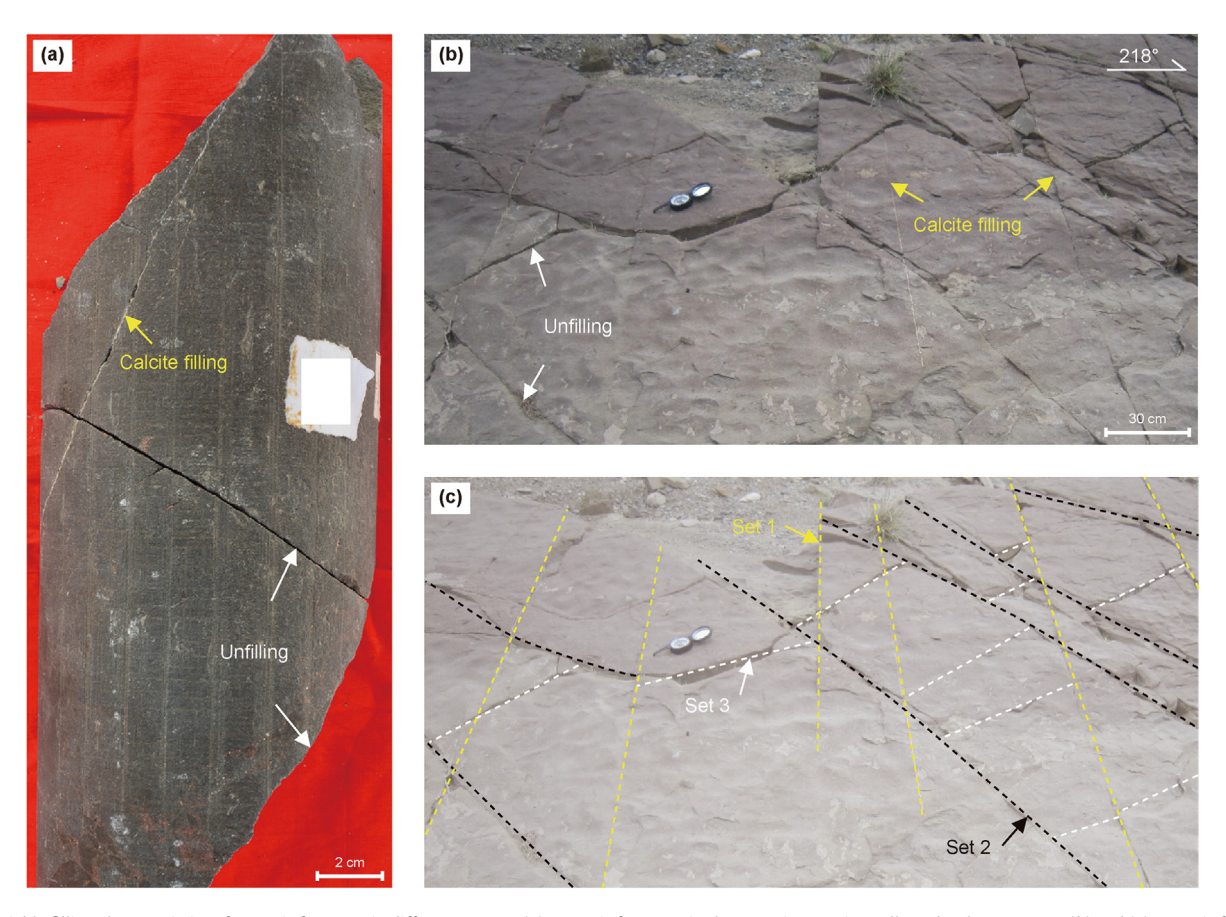


Fig. 14. Variable filling characteristics of tectonic fractures in different groups. (a) Tectonic fractures in the Jurassic cores in Well B9, depth 1856.50 m, (b) and (c) tectonic fractures in the Jurassic outcrops. Set 1 is NW-SE striking fractures. Set 2 is NEE-SWW striking fractures.

control of cementation and dissolution on the effectiveness of natural fractures in deep tight sandstone reservoirs, while other diagenesis, such as compression and abnormally high pressure, may also affect fracture effectiveness. The type and intensity of cementation experienced by natural fractures are consistent with the reservoir pores, causing them to be filled to varying degrees and reducing their effectiveness (Lai et al., 2023a,b). In the Jurassic tight sandstone reservoirs of the foreland thrust belt in the southern Junggar Basin, the eastern section belongs to the strongly cemented diagenetic facies, in which tectonic fractures have the highest filling degree and more than 40% of them are filled with minerals to

varying degrees. Reservoirs in the middle and western sections are moderately to weakly cemented diagenetic facies, and mineral-filled fractures account for 28.1% and 23.6%, respectively. Furthermore, the proportion of fractures with different filling degrees also changes in these structural units (Fig. 16). The eastern section has the highest proportion of partial-filled fractures, while the middle and western sections own the largest proportion of complete-filled fractures, accounting for nearly half of all mineral-filled fractures. These results manifest that cementation in reservoir evolution is detrimental to the effectiveness of natural fractures, and the

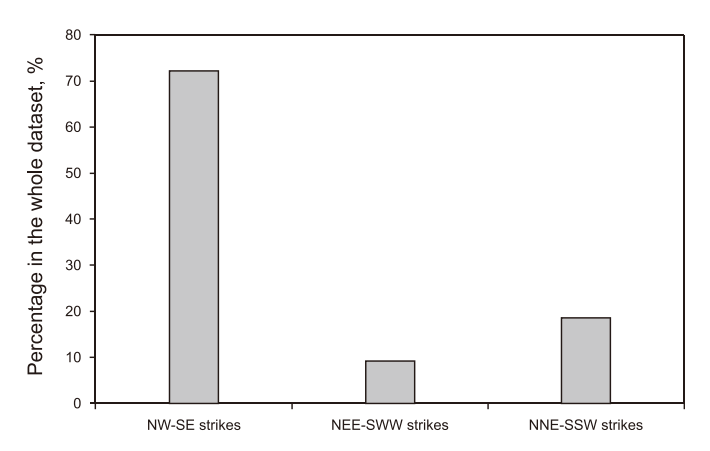


Fig. 15. The proportion of different groups in mineral-filled tectonic fractures of the Jurassic outcrops.

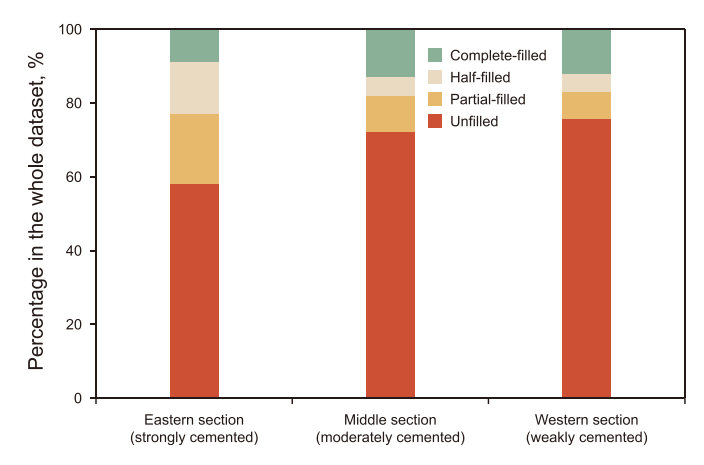


Fig. 16. The proportion of tectonic fractures with varying filling degrees from the Jurassic cores in different sections of the southern Junggar Basin.

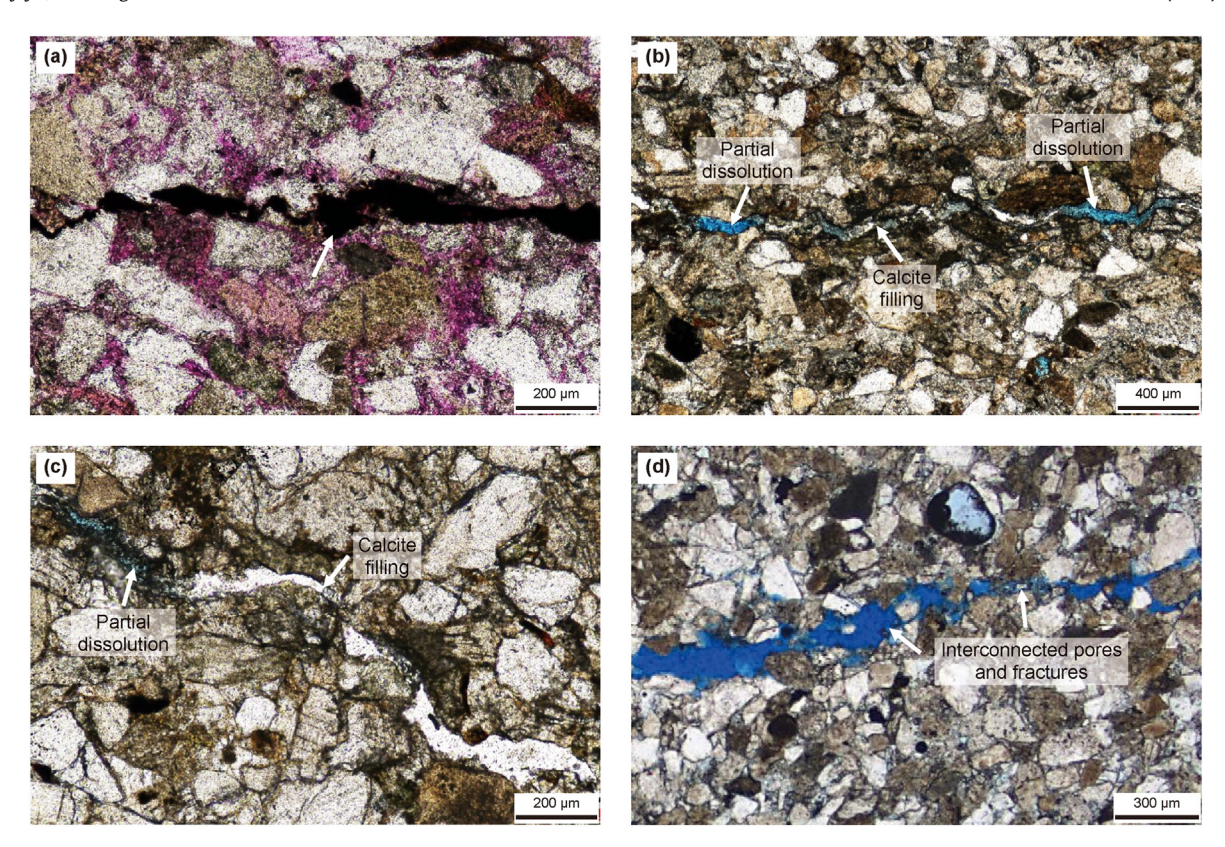


Fig. 17. Natural fractures affected by dissolution in the Jurassic thin sections. (a) Well B12, depth 4350.50 m (Modified from Liu et al., 2020b). (b) Well B5, depth 5841.25 m. (c) Well B3, depth 5408.21 m. (d) Well B21, depth 2613.02 m.

difference in the degree of cementation would be an essential factor controlling fracture effectiveness.

In addition, deep tight sandstone reservoirs have experienced different intensities of dissolution during diagenetic evolution, which also affects the effectiveness of natural fractures. Dissolution caused by reservoir fluids can transform natural fractures that are not filled with minerals, making their surface curved and irregular (Fig. 17(a)). This dissolution transformation increases the fracture aperture and makes the aperture in different parts notably different. Besides, reservoir fluids can partially or completely dissolve the minerals in fractures, making the mineral-filled fractures effective again (Fig. 17(b) and (c)). Such dissolved minerals in these filled fractures are mainly calcite, in addition to a small amount of clay minerals. There are usually many interconnecting multiple dissolution pores developed near the fractures transformed by dissolution, which enhances the connectivity of the reservoir storage space (Nelson, 2001) (Fig. 17(d)). Therefore, dissolution is beneficial to improving the effectiveness of natural fractures in deep tight sandstone reservoirs.

6. Conclusions

Tectonic fractures are the dominant type of natural fractures in deep tight sandstone reservoirs of foreland thrust belts. Spanning from the eastern to western sections and extending from the near Tianshan orogen to the interior Junggar Basin, the intensity of tectonic activities and resulting deformations are gradually weakened, which leads to a decrease in the dominant fracture groups and a reduction in their scale and density. Moreover, the intense tectonic deformation in the foreland thrust belt causes large changes in the stratum occurrence, resulting in a wide range of the fracture's dip angles. These differential distribution results would

refine the development patterns of natural fractures in deep tight sandstone reservoirs of the foreland thrust belt.

The evolution of deep tight sandstone reservoirs in foreland thrust belts is a complex process where tectonism and diagenesis play a crucial role in controlling fracture effectiveness. The control of tectonism is evident in the fact that NW-SE striking fractures formed in earlier stages are more likely to be filled with minerals, causing their effectiveness to deteriorate significantly, while the NEE-SWW and NNE-SSW striking fractures are formed later and therefore have less filling and are more effective. In addition, cementation causes fractures to be filled with minerals, becoming barriers to fluid flow and adversely affecting the fracture effectiveness. However, dissolution is beneficial to improving their effectiveness by increasing fracture aperture and their connectivity to pores. These insights would contribute to revealing the evolutionary mechanisms of fracture effectiveness in deep tight sandstone reservoirs of foreland thrust belts.

CRediT authorship contribution statement

Guo-Ping Liu: Writing — original draft, Investigation, Formal analysis, Conceptualization. **Zhi-Jun Jin:** Writing — review & editing, Supervision. **Lian-Bo Zeng:** Writing — review & editing, Supervision, Project administration.

Declaration of competing interest

The authors declare that they have no known competing financial interests or personal relationships that could have appeared to influence the work reported in this paper.

Acknowledgments

This study is supported by the CNPC Innovation Found (No. 2023DQ02-0103) and National Major Science and Technology Projects of China (No. 2016ZX05003-001). The authors greatly acknowledge the editors and anonymous reviewers for their constructive comments and rigorous review, which will contribute significantly to improving this manuscript.

References

- Ajdukiewicz, J.M., Nicholson, P.H., Esch, W.L., 2010. Prediction of deep reservoir quality from early diagenetic process models in the Jurassic eolian Norphlet Formation, Gulf of Mexico. AAPG Bull. 94 (8), 1189–1227. https://doi.org/10.1306/04211009152.
- Aguilera, R., 1998. Formation evaluation of triassic naturally fractured carbonates in British Columbia. J. Can. Petrol. Technol. 37 (7), 23–33. https://doi.org/10.2118/98-07-02.
- Azizmohammadi, S., Matthäi, S.K., 2017. Is the permeability of naturally fractured rocks scale dependent? Water Resour. Res. 53 (9), 8041–8063. https://doi.org/10.1002/2016WR019764.
- Branellec, M., Callot, J.P., Aubourg, C., Niviere, B., Ringenbach, J.C., 2015. Matrix deformation in a basement-involved fold-and-thrust-belt: a case study in the central Andes, Malargue (Argentina). Tectonophysics 658, 186–205. https://doi.org/10.1016/j.tecto.2015.07.022.
- Bush, M.A., Horton, B.K., Murphy, M.A., Stockli, D.F., 2016. Detrital record of initial basement exhumation along the Laramide deformation front, southern Rocky Mountains. Tectonics 35 (9), 2117–2130. https://doi.org/10.1002/2016TC004194.
- Cai, J., Lu, X.X., Li, B.Y., 2016. Tectonic fracture and its significance in hydrocarbon migration and accumulation: a case study on middle and lower Ordovician in Tabei Uplift of Tarim Basin, NW China. Geol. J. 51 (4), 572–583. https://doi.org/ 10.1002/gi.2656.
- Cao, J., Wang, X.L., Wei, D.T., Sun, P.A., Hu, W.X., Jia, D., Zhao, Y.C., 2010. Complex petroleum migration and accumulation in central region of southern Junggar Basin, northwest China. J. Earth Sci-China. 21 (1), 83–93. https://doi.org/10.1007/s12583-010-0004-5.
- Cardozo, N., Allmendinger, R.W., Morgan, J.K., 2005. Influence of mechanical stratigraphy and initial stress state on the formation of two fault propagation folds. J. Struct. Geol. 27, 1954–1972. https://doi.org/10.1016/j.jsg.2005.06.003.
- Chapman, J.B., Chapman, P.G., 2015. Foreland basin stratigraphic control on thrust belt evolution. Geology 43 (7), 579–582. https://doi.org/10.1130/G36597.1.
- Clayton, J.L., Yang, J., King, J.D., Lillis, P.G., Warden, A., 1997. Geochemistry of oils from the Junggar basin, northwest China. AAPG Bull. 81 (11), 1926–1944. https://doi.org/10.1306/3B05C672-172A-11D7-8645000102C1865D.
- Ding, W.L., Dai, P., Zhu, D.W., Zhang, Y.Q., He, J.H., Li, A., Wang, R.Y., 2016. Fractures in continental shale reservoirs: a case study of the Upper Triassic strata in the SE Ordos Basin, Central China. Geol. Mag. 153 (4), 663–680. https://doi.org/ 10.1017/S001675681500062X.
- Ding, W.L., Li, C., Li, C.Y., Xu, C.C., Jiu, K., Zeng, W.T., Wu, L.M., 2012. Fracture development in shale and its relationship to gas accumulation. Geosci. Front. 3 (1), 97–105. https://doi.org/10.1016/j.gsf.2011.10.001.
 Eckert, A., Connolly, P., Liu, X., 2014. Large-scale mechanical buckle fold develop-
- Eckert, A., Connolly, P., Liu, X., 2014. Large-scale mechanical buckle fold development and the initiation of tensile fractures. Geochem. Geophy. Geosy. 15 (11), 4570–4587. https://doi.org/10.1002/2014gc005502.
- Ehrenberg, S.N., Nadeau, P.H., 2005. Sandstone vs. carbonate petroleum reservoirs: a global perspective on porosity-depth and porosity-permeability relationships. AAPG Bull. 89 (4), 435–445. https://doi.org/10.1306/11230404071.
- Eichhubl, P., Davatz, N.C., Becker, S.P., 2009. Structural and diagenetic control of fluid migration and cementation along the Moab fault, Utah. AAPG Bull. 93 (5), 653–681. https://doi.org/10.1306/02180908080.
- Eude, A., Roddaz, M., Brichau, S., Brusset, S., Calderon, Y., Baby, P., Soula, J.C., 2015. Controls on timing of exhumation and deformation in the northern Peruvian eastern Andean wedge as inferred from low-temperature thermochronology and balanced cross section. Tectonics 34 (4), 715–730. https://doi.org/10.1002/ 2014TC003641.
- Feng, J.W., Qu, J.H., Wan, H.Q., Ren, Q.Q., 2021. Quantitative prediction of multiperiod fracture distributions in the cambrian-ordovician buried hill within the futai oilfield, jiyang depression, east China. J. Struct. Geol. 148, 104359. https://doi.org/10.1016/j.jsg.2021.104359.
- Feng, J.W., Ren, Q.Q., Xu, K., 2018. Quantitative prediction of fracture distribution using geomechanical method within Kuqa Depression, Tarim Basin, NW China. J. Petrol. Sci. Eng. 162, 22—34. https://doi.org/10.1016/j.petrol.2017.12.006. Fossen, H., Schultz, R.A., Shipton, Z.K., Mair, K., 2007. Deformation bands in sand-
- Fossen, H., Schultz, R.A., Shipton, Z.K., Mair, K., 2007. Deformation bands in sandstone: a review. J. Geol. Soc. 164 (4), 755–769. https://doi.org/10.1144/0016-76492006-036.
- Gale, J.F.W., Lander, R.H., Reed, R.M., Laubach, S.E., 2010. Modeling fracture porosity evolution in dolostone. J. Struct. Geol. 32 (9), 1201–1211. https://doi.org/10.1016/j.jsg.2009.04.018.
- Gomez-Rivas, E., Butler, R.W.H., Healy, D., Alsop, G.I., 2020. From hot to cold the temperature dependence on rock deformation processes: an introduction. J. Struct. Geol. 132, 103977. https://doi.org/10.1016/j.jsg.2020.103977.

Gong, L., Gao, M.Z., Zeng, L.B., Fu, X., Gao, Z., Gao, A., Zu, K., Yao, J., 2017. Controlling factors on fracture development in the tight sandstone reservoirs: a cases tudy of Jurassic-Neogene in the Kuqa foreland basin. Nat. Gas Geosci. 28 (2), 199–208. https://doi.org/10.11764/j.issn.16721926.2016.12.003 (in Chinese).

- Guan, S.W., Stockmeyer, J.M., Shaw, J.H., Plesch, A., Zhang, J., 2016. Structural inversion, imbricate wedging, and out-of-sequence thrusting in the southern Junggar fold-and-thrust belt, northern Tian Shan, China. AAPG Bull. 100 (9), 1443–1468. https://doi.org/10.1306/04041615023.
- Guo, Z.J., Wu, C.D., Zhang, Z.C., Chen, W., 2011. Tectonic control on hydrocarbon accumulation and prospect for large oil-gas field exploration in the southern Junggar Basin. Geol. J. China Univ. 17, 185–195. https://doi.org/10.1007/s12182-011-0118-0 (in Chinese).
- Hannah, W., Robert, W.H.B., Clare, E.B., Dave, H., 2015. Influence of structural position on fracture networks in the Torridon Group, Achnashellach fold and thrust belt, NW Scotland. J. Struct. Geol. 74, 64–80. https://doi.org/10.1016/j.jsg.2015.03.001.
- Hennings, P.H., Olson, J.E., Thompson, L.B., 2000. Combining outcrop data and three-dimensional structural models to characterize fractured reservoirs: an example from Wyoming. AAPG Bull. 84 (6), 830–884. https://doi.org/10.1306/a967340a-1738-11d7-8645000102c1865d.
- Hernandez, M., Franzese, J.R., 2017. The fracture patterns of the Tin anticline: fracturing process during the foreland evolution in the Calchaqui Valley, northwestern Argentina. J. Struct. Geol. 96, 54–64. https://doi.org/10.1016/j.jsg.2017.01.011.
- Hong, F., Jiang, L., Zhuo, Q.G., Lu, X.S., Ma, X.Z., Hao, J.Q., 2018. Types of abnormal high-pressure gas reservoir in foreland basins of China. Nat. Gas Geosci. 29 (3), 317–327. https://doi.org/10.11764/j.issn.1672-1926.2018.02.003 (in Chinese).
- Hood, S.D., Nelson, C.S., Kamp, J.J., 2003. Modification of fracture porosity by multiphase vein mineralization in an oligocene nontropical carbonate reservoir, Taranaki Basin, New Zealand. AAPG Bull. 87 (10), 1575–1597. https://doi.org/ 10.1306/06040301103.
- Hu, H.W., Tian, X.R., Zhang, J., Zhuo, Q.G., Jia, C.Z., Guo, Z.J., 2010. The diagenetic and tectonic significance of hydrocarbon accumulation in the southern Junggar Basin, NW China. Geol. J. 53 (6), 2795–2809. https://doi.org/10.1002/gj.3119.
- Ju, W., Hou, G., Li, L., Xiao, F.F., 2012. End Late Paleozoic tectonic stress field in the southern edge of Junggar Basin. Geosci. Front. 3 (5), 707–715. https://doi.org/ 10.1016/j.gsf.2011.12.007.
- Ju, W., Wang, K., Hou, G., Sun, W., Yu, X., 2018. Prediction of natural fractures in the lower jurassic ahe formation of the dibei gasfield, kuqa depression, tarim basin, NW China. Geosci. J. 22 (2), 241–252. https://doi.org/10.1007/s12303-017-0039-7
- Kerimov, V.Y., Leonov, M.G., Mustaev, R.N., Hai, V.N., 2019. Hydrocarbons in the basement of the south China sea (vietnam) shelf and structural-tectonic model of their formation. Geotectonics 53 (1), 42–59. https://doi.org/10.1134/ S0016852119010035.
- Kranz, R.L., 1983. Microcracks in rocks: a review. Tectonophysics 100 (1–3), 449–480. https://doi.org/10.1016/0040-1951(83)90198-1.
- Kus, J., 2017. Oxidatively and thermally altered high-volatile bituminous coals in high-temperature coal fire zone No. 8 of the Wuda Coalfield (North China). Int. J. Coal Geol. 176, 8–35. https://doi.org/10.1016/j.coal.2017.04.006.
- Lahiri, S., 2021. Estimating effective permeability using connectivity and branch length distribution of fracture network. J. Struct. Geol. 146, 104314. https:// doi.org/10.1016/j.jsg.2021.104314.
- Lai, J., Li, D., Bai, T.Y., Zhao, F., Ai, Y., Liu, H.K., Cai, D.Y., Wang, G.W., Chen, K.J., Xie, Y.Q., 2023a. Reservoir quality evaluation and prediction in ultra-deep tight sandstones in the Kuqa depression, China. J. Struct. Geol. 170, 104850. https:// doi.org/10.1016/j.jsg.2023.104850.
- Lai, J., Zhao, F., Zhang, M., Bai, T., Huang, Y., Li, D., Wang, G., Qin, Z., 2023b. How high can fracture porosity become in the ultra-deep subsurface? Geosci. Front. 14 (5), 101617. https://doi.org/10.1016/j.gsf.2023.101617.
- Landry, C.J., Eichhubl, P., Prodanovic, M., Wilkins, S., 2016. Nanoscale grain boundary channels in fracture cement enhance flow in mudrocks. J. Geophys. Res. Solid Earth 121 (5), 3366–3376. https://doi.org/10.1002/2016JB012810.
- Laubach, S.E., Eichhubl, P., Hilgers, C., Lander, R.H., 2010. Structural diagenesis.
 J. Struct. Geol. 32 (12), 1866—1872. https://doi.org/10.1016/j.jsg.2010.10.001.
- Laubach, S.E., Olson, J.E., Gross, M.R., 2009. Mechanical and fracture stratigraphy. AAPG Bull. 93 (11), 1413–1426. https://doi.org/10.1306/07270909094.
- Li, Y.J., Wang, T.D., Zhang, Y.Y., Chen, S.J., Wang, X.L., 2004. Natural gas genesis and formation of gas pools in the south margin of Junggar Basin. Acta Sedimantologica Sin 22, 529–534. https://doi.org/10.14027/j.cnki.cjxb.2004.03.024 (in Chinese)
- Liu, G.P., Jin, Z.J., Zeng, L.B., Chen, X.X., Mehdi, O., Wang, Q.Q., Lu, G.Q., Du, X.Y., 2025. Laminar controls on bedding-parallel fractures in Permian lacustrine shales, Junggar Basin, northwestern China. Geol. Soc. Am. Bull. 137 (7–8), 3512–3526. https://doi.org/10.1130/B37792.1.
- Liu, G.P., Zeng, L.B., Han, C.Y., Mehdi, O., Lyu, W.Y., Wang, Q.Q., Zhu, J.W., Hou, F.X., 2020a. Natural fractures in carbonate basement reservoirs of the Jizhong Sub-Basin, Bohai Bay Basin, China: key aspects favoring oil production. Energies 13 (18), 4635. https://doi.org/10.3390/en13184635.
- Liu, G.P., Zeng, L.B., Wang, X.J., Mehdi, O., Wang, Z.L., Mao, Z., Tie, Q., 2020b. Natural fractures in deep tight gas sandstone reservoirs in the thrust belt of the southern Junggar Basin, northwestern China. Interpretation 8 (4), 81–93. https://doi.org/10.1190/int-2020-0051.1.
- Liu, G.P., Zeng, L.B., Zhu, R.K., Gong, L., Mehdi, O., Mao, Z., 2021. Effective fractures and their contribution to the reservoirs in deep tight sandstones in the Kuqa

- Depression, Tarim Basin, China. Mar. Petrol. Geol. 124, 104824. https://doi.org/10.1016/j.marpetgeo.2020.104824.
- Liu, J.S., Ding, W.L., Yang, H.M., Jiu, K., Wang, Z., Li, A., 2018. Quantitative prediction of fractures using the finite element method: a case study of the lower Silurian Longmaxi Formation in northern Guizhou, South China. J. Asian Earth Sci. 154, 397–418. https://doi.org/10.1016/j.jseaes.2017.12.038.
- Liu, J.S., Lu, Y.H., Xu, K., Luo, Y., Yang, H.M., Lu, L., 2024. Main controlling factors and prediction model of fracture scale in tight sandstone: insights from dynamic reservoir data and geomechanical model analysis. Rock Mech. Rock Eng. 57 (10), 8343–8362. https://doi.org/10.1007/s00603-024-03979-3.
- Lyu, W., Zeng, L., Zhang, B., Miao, F., Lyu, P., Dong, S., 2017. Influence of natural fractures on gas accumulation in the Upper Triassic tight gas sandstones in the northwestern Sichuan Basin, China. Mar. Petrol. Geol. 83, 60–72. https://doi.org/10.1016/j.marpetgeo.2017.03.004.
- Machel, H.G., Cavell, P.A., Patey, K.S., 1996. Isotopic evidence for carbonate cementation and recrystallization, and for tectonic expulsion of fluids into the Western Canada Sedimentary Basin. Geol. Soc. Am. Bull. 108 (9), 1108–1119. https://doi.org/10.1130/0016-7606(1996)108<1108:1EFCCA>2.3.CO:2.
- Mao, Z., Zeng, L.B., Liu, G.D., Liu, G.P., Tian, H., Dong, S.Q., Lyu, W.Y., Mehdi, O., 2022.
 Controls of fault-bend fold on natural fractures: insight from discrete element simulation and outcrops in the southern margin of the Junggar Basin, Western China. Mar. Petrol. Geol. 138, 105541. https://doi.org/10.1016/j.marpetgeo.2022.105541.
- Mao, Z., Zeng, L.B., Liu, G.P., Tian, H., Liao, Q., Zhang, Y.Z., 2020. Characterization and effectiveness of natural fractures in deep tight sandstones at the south margin of the Junggar Basin, northwestern China. Oil Gas Geol. 41 (6), 1212–1221. https://doi.org/10.11743/ogg20200609 (in Chinese).
- Meng, Q., Hao, F., Tian, J., 2021. Origins of non-tectonic fractures in shale. Earth Sci. Rev. 222, 103825. https://doi.org/10.1016/j.earscirev.2021.103825.
- Nelson, R.A., 2001. Geologic Analysis of Naturally Fractured Reservoirs, second ed. Gulf Professional Publishing, Butterworth-Heinemann, p. 332.
- Ortega, O.J., Marrett, R.A., Laubach, S.E., 2006. A scale-independent approach to fracture intensity and average spacing measurement. AAPG Bull. 90 (2), 193–208. https://doi.org/10.1306/08250505059.
- Qiu, Z.K., He, N.X., Wang, H., Li, X., Li, T., Zhou, Q., Wu, X., Shi, L., 2021. The sedimentological reservoir characteristics of the jurassic Sangonghe formation, southern mahu slope, Junggar Basin, northwestern China. Geol. J. 56 (3), 1478–1495. https://doi.org/10.1002/gj.4014.
- Rachinskiy, M.Z., Chilingar, G.V., Gorfunkel, M.V., 2007. Oil and gas potential of south-Caspian basin. Energy Sources, Part A Recovery, Util. Environ. Eff. 29 (15), 1339–1360. https://doi.org/10.1080/15567030701545964.
- Ramsey, J.M., Chester, F.M., 2002. Hybrid fracture and the transition from extension fracture to shear fracture. Nature 1773, 2002–2005. https://doi.org/10.1038/ nature02333.
- Sanz, P.F., Pollard, D.D., Allwardt, P.F., Borja, R.I., 2008. Mechanical models of fracture reactivation and slip on bedding surfaces during folding of the asymmetric anticline at Sheep Mountain, Wyoming. J. Struct. Geol. 30 (9), 1177–1191. https://doi.org/10.1016/j.jsg.2008.06.002.
- Selvadurai, A.P.S., Zhang, D.J., Kang, Y.L., 2018. Permeability evolution in natural fractures and their potential influence on loss of productivity in ultra-deep gas reservoirs of the Tarim Basin, China. J. Nat. Gas Sci. Eng. 58, 162–177. https://doi.org/10.1016/j.jngse.2018.07.026.
- Sun, Z.M., He, Z.L., Mou, Z.H., 2004. Structural features and favorable exploration areas in southern margin of Junggar basin. Oil Gas Geol. 25, 216–221. https:// doi.org/10.11743/ogg20040217 (in Chinese).
- Tavani, S., Storti, F., Lacombe, O., Corradetti, A., Muñoz, J.A., Mazzoli, S., 2015. A review of deformation pattern templates in foreland basin systems and fold-and-thrust belts: implications for the state of stress in the frontal regions of thrust wedges. Earth Sci. Rev. 141, 82–104. https://doi.org/10.1016/j.earscirev.2014.11.013.
- Wan, Z.F., Shi, Q.H., Zhang, Q., Cai, S., Xia, B., 2015. Characteristics and developmental mechanisms of mud volcanoes on the southern margin of the Junggar Basin, NW China. Geol. J. 50, 434–445. https://doi.org/10.1002/gj.2547.
- Wang, Q., Laubach, S.E., Gale, J., Ramos, M.J., 2019. Quantified fracture (joint) clustering in archean basement, Wyoming: application of normalized correlation count method. Pet. Geosci. 25 (4), 415–428. https://doi.org/10.1144/pet-geo2018-146.
- Wang, Y.L., Liu, X.G., 2021. Stress-Dependent unstable dynamic propagation of three-dimensional multiple hydraulic fractures with improved fracturing

- sequences in heterogeneous reservoirs: numerical cases study via poroelastic effective medium model. Energy Fuels 35 (22), 18543—18562. https://doi.org/10.1021/acs.energyfuels.1c03132.
- Warpinski, N.R., Teufel, L.W., 1987. Influence of geologic discontinuities on hydraulic fracture propagation. J. Petrol. Technol. 39 (2), 209–220. https://doi.org/ 10.2118/13224-PA.
- Watkins, H., Butler, R.W.H., Bond, C.E., Healy, D., 2015. Influence of structural position on fracture networks in the Torridon Group, Achnashellach fold and thrust belt, NW Scotland. J. Struct. Geol. 74, 64–80. https://doi.org/10.1016/j.isg.2015.03.001.
- Wierzbicki, R., Dravis, J.J., Al-Aasm, I., Harland, N., 2006. Burial dolomitization and dissolution of upper jurassic Abenaki platform carbonates, deep panuke reservoir, nova scotia, Canada. AAPG Bull. 90 (11), 1843–1861. https://doi.org/ 10.1306/03200605074.
- Yang, Y.T., Song, C.C., He, S., 2015. Jurassic tectonostratigraphic evolution of the Junggar basin, NW China: a record of Mesozoic intraplate deformation in Central Asia. Tectonics 34 (1), 86–115. https://doi.org/10.1002/2014TC003640.
- Yu, F.S., Li, G.Z., Yang, G.D., Ma, B.J., Chen, S.P., 2009. Deformation feature and genesis simulation of fold-and-thrust belts in the southern margin Junggar Basin. Geotect. Metallogenia 33 (3), 386–395. https://doi.org/10.16539/j.ddgzyckx.2009.03.006 (in Chinese).
- Zeng, L., Jiang, J.W., Yang, Y.L., 2010. Fractures in the low porosity and ultra-low permeability glutenite reservoirs: a case study of the late Eocene Hetaoyuan formation in the Anpeng Oilfield, Nanxiang Basin, China, Mar. Petrol. Geol. 27, 1642–1650. https://doi.org/10.1016/j.marpetgeo.2010.03.009.
- Zeng, L.B., Li, X.Y., 2009. Fractures in sandstone reservoirs with ultra-low permeability: a case study of the upper Triassic Yanchang Formation in the Ordos basin, China. AAPG Bull. 93 (4), 461–477. https://doi.org/10.1306/09240808047.
- Zeng, L.B., Lyu, W.Y., Li, J., Zhu, L., Weng, J., Yue, F., Zu, K., 2016. Natural fractures and their influence on shale gas enrichment in Sichuan Basin, China. J. Nat. Gas Sci. Eng. 30, 1–9. https://doi.org/10.1016/j.jngse.2015.11.048.
- Zeng, L., Tang, X., Wang, T., Gong, L., 2012. The influence of fracture cements in tight Paleogene saline lacustrine carbonate reservoirs, western Qaidam Basin, northwest China. AAPG Bull. 96 (11), 2003–2017. https://doi.org/10.1306/ 04181211090
- Zhang, C., Zhu, D.Y., Luo, Q., Liu, L.F., Liu, D.D., Yan, L., Zhang, Y.Z., 2017. Major factors controlling fracture development in the Middle Permian Lucaogou Formation tight oil reservoir, Junggar Basin, NW China. J. Asian Earth Sci. 146, 279–295. https://doi.org/10.1016/j.jseaes.2017.04.032.
- Zhang, H.H., Zhang, Z.C., Tang, W.H., Li, K., Li, J.F., Wang, Q., Ding, C., 2022. Burial and exhumation history of Jurassic sedimentary rocks in the southern margin of the Junggar Basin: implications for the growth of the northern Tianshan Mountains. J. Asian Earth Sci. 236, 105339. https://doi.org/10.1016/j.jseaes.2022.105339.
- Zhang, H.L., Zhang, R.H., Yang, H.J., Shou, J.F., Wang, J.P., Liu, C., Chen, G., 2014. Characterization and evaluation of ultra-deep fracture-pore tight sandstone reservoirs: a case study of Cretaceous Bashijiqike Formation in Kelasu tectonic zone in Kuqa foreland basin, Tarim, NW China. Petrol. Explor. Dev. 41 (2), 175–184. https://doi.org/10.1016/S1876-3804(14)60020-3.
- Zhang, W., Zhang, B.L., Zhao, T.B., 2023. Study on the law of failure acoustic-thermal signal of weakly cemented fractured rock with different dip angles. Rock Mech. Rock Eng. 56 (6), 4557–4568. https://doi.org/10.1007/s00603-023-03296-1.
- Zhang, Z.Y., Zhu, G.Y., Chi, L.X., Wang, P.J., Zhou, L., Li, J.F., Wu, Z.H., 2020. Discovery of the high -yield well GT1 in the deep strata of the southern margin of the Junggar Basin, China: implications for liquid petroleum potential in deep assemblage. J. Petrol. Sci. Eng. 191, 107178. https://doi.org/10.1016/j.petrol.2020.107178.
- Zhao, G.P., 2003. Overpressure and its relation to petroleum accumulation in southern edge of Junggar Basin. Oil Gas Geol. 24 (4), 327–331. https://doi.org/ 10.3321/j.issn:0253-9985.2003.04.004 (in Chinese).
- Zhou, T.Q., Wu, C.D., Guan, X.T., Wang, J.L., Jiao, Y., 2022. Coupling relationship between reservoir densification and hydrocarbon emplacement in the Jurassic Badaowan Formation sandstone reservoirs of the southern Junggar Basin, China. Geol. J. 57 (7), 2473–2496. https://doi.org/10.1002/gj.4429.
- Zhu, G.Y., Chen, W.Y., Yan, H.H., Yan, L., Zhang, Z.Y., Zhao, K., Li, T.T., 2022. Sinian tectonic evolution and distribution of source rocks in northwest Tarim Basin, China. Mar. Petrol. Geol. 144 (1), 105826. https://doi.org/10.1016/j.marpetgeo.2022.105826.